

Modelling of the substrate heterogeneities experienced by a limited microbial population in scale-down and in large-scale bioreactors

F. Delvigne^{a,*}, A. Lejeune^a, J. Destain^a, P. Thonart^{a,b,1}

^a Centre Wallon de Biologie Industrielle, Unité de Bio-industries, Faculté des Sciences Agronomiques de Gembloux, Passage des déportés, 2, B-5030 Gembloux, Belgium

^b Centre Wallon de Biologie Industrielle, Service de Technologie Microbienne, Université de Liège, Sart-Tilman, B40, B-4000 Liège, Belgium

Received 12 September 2005; received in revised form 29 March 2006; accepted 30 March 2006

Abstract

A methodology based on stochastic modelling is presented to describe the influence of the bioreactor heterogeneity on the microorganisms growth and physiology. The stochastic model is composed of two sub-models: a microorganism circulation sub-model and a fluid mixing sub-model used for the characterization of the concentration gradient. The first one is expressed by a classical stochastic model (with random number generation), whereas the second one is expressed by a stochastic Markov chain. Their superimposition permits to obtain the concentration profiles experienced by the microorganisms in the bioreactor. The simulation results are expressed in the form of frequency distributions. At first, the study has been focused on the design of scale-down reactors (SDR). This kind of reactor has been reported to be an efficient tool to study at a small-scale the hydrodynamic behaviour encountered in large-scale reactor [P. Neubauer, L. Horvat, S.O. Enfors, Influence of substrate oscillations on acetate formation and growth yield in *Escherichia coli* glucose limited fed-batch cultivations, *Biotechnol. Bioeng.* 47 (1995) 139–146]. Several parameters affecting the shape of the frequency distributions have been tested. Among these, it appears that the perturbation frequency, the exposure time and the design of the non-mixed part of the SDR have a significant influence on the shape of the distributions. The respective influence of all these parameters must be taken into account in order to obtain representative results. As a general trend, the increase of the recirculation flow rate between the mixed and the non-mixed part of the SDR induce a shift of the frequency distribution for the lower relative concentrations, which suggests an attenuation of the scale-down effect. This has been validated by using the SDR in the case of the cultivation of *Saccharomyces cerevisiae*. However, the influence of the non-mixed part of the SDR is not quite well understood if only taking account of the frequency distribution analysis, and supplementary experiments are required to elucidate the underlying mechanism.

The aspect of the frequency distributions suggests that both the design and the operating conditions of a scale-down reactor need to be adjusted in order to match the behaviour of a given large-scale reactor. Examples of frequency distributions obtained in the case of large-scale reactors are given. © 2006 Elsevier B.V. All rights reserved.

Keywords: Scale-down; Stochastic; Modelling

1. Introduction

Structured compartment models have been widely used to describe the hydrodynamics of stirred bioreactors [2–5]. They are generally mathematically expressed by a set of ordinary differential equations. Recently, stochastic models, already well described for particulate mixing applications [6,7], have been developed in the case of fluid mixing in stirred bioreactors [8]. This kind of model has shown good results if compared with the classical deterministic compartment models. The main advan-

tage lies on the fact that the stochastic models can be used both for fluid mixing and particle circulation simulation. The superimposition of the two mechanisms (i.e. fluid mixing and particle circulation) permits to obtain the concentration profiles experienced by microorganisms inside bioreactors. These profiles can be used to elucidate some fluid mechanics impacts on the microbial physiology. Indeed, the reactor heterogeneities do have a significant influence on the microorganisms physiology. This physiological change depends on the kind of microorganism considered, for example:

- In the case of *Escherichia coli*, spatial heterogeneities of glucose induce an overflow metabolism, which leads to the formation of acetate [1,9]. On the other hand, the passage of

* Corresponding author. Tel.: +32 81 62 23 11; fax: +32 81 61 42 22.

E-mail address: bioindus@fsagx.ac.be (F. Delvigne).

¹ Tel.: +32 4 366 28 61; fax: +32 4 366 28 62.

Nomenclature

d	impeller diameter (m)
D	vessel diameter (m)
N	stirred speed (s^{-1})
N_{qc}	circulation flow number (dimensionless)
P	probability to achieve a given displacement in the stochastic model
Q_c	circulation flow rate (m^3/s)
S	state vector of a Markov chain stochastic model
S_0	initial state vector
S_{pulse}	matrix expressing the fed-batch pump pulses frequency
SDR	scale-down reactor
T	transition matrix of the stochastic model
u_g	gas superficial velocity (m/s)
<i>Greek letters</i>	
ρ_g	density of the gas phase (kg/m^3)
ρ_l	density of the liquid phase (kg/m^3)

E. coli in oxygen depleted zones induces a mixed acid fermentation metabolism [9].

- In the case of *Saccharomyces cerevisiae*, spatial heterogeneities of glucose also induces an overflow metabolism traduced by the formation of ethanol [10–12].

When scaling-up a bioreactor, the homogenization efficiency drops, which leads to the appearance of concentration gradient. In addition, the way in which microorganisms are exposed to this gradient evolves, on account of to the multiplication of the possible circulation paths while increasing the reactor volume. This phenomena can be represented by an increase of the variance of the corresponding circulation time distribution. In this way, the use of a model allowing the description of the extracellular substrate concentrations experienced by the microorganisms seems to be an efficient tool to elucidate the bioreactor effect on its biotic phase (constituted by the whole microbial population in the reactor).

Firstly, stochastic models as presented in this study will be used to characterize the mixing and circulation behaviours in scale-down reactors (SDR). This kind of reactor generally comprises a mixed part connected to a non-mixed part [1]. The recirculation of the liquid through the non-mixed loop of the reactor leads to the formation of concentration gradient. SDR is an efficient tool to study at small scale the fluid dynamic characteristics encountered in large-scale reactors. Secondly, the stochastic modelling methodology will be used in the case of large-scale reactors.

2. Material and methods

2.1. Scale-down reactor configuration

The scale-down reactor comprises a mixed part and a non-mixed one. The mixed part consists of a 20l stirred bioreactor

($D=0.22$ m; working volume: 10 l) equipped with a rushton disk turbine with six blades ($d=0.1$ m).

The design of the non-mixed part can be adapted. In this study, two configurations have been tested:

- Configuration A (SDR type A): the non-mixed part consists of a glass bulb (i.d.: 85 mm; length: 0.25 m; connections of 8 mm diameter at each end).
- Configuration B (SDR type B): the non-mixed part consists of a silicone tubing (i.d.: 8 mm; length: 7.5 m).

The liquid flow between the two parts of the SDR is ensured by a peristaltic pump (Watson Marlow 323 SD).

2.2. Large-scale bioreactors configurations

Two kinds of large-scale reactors have been investigated:

- A 2 m^3 stirred bioreactor (D : 1 m; working volume: 1800 l; three agitation stages; rushton disk turbine with four blades; d : 0.45 m).
- A 9 m^3 bubble column bioreactor (D : 2 m; working volume: 9000 l).

2.3. Inert tracer test

Mixing experiments have been performed both in scale-down reactor and in large-scale reactors by a tracer pulse injection method. The technique consists in measuring the conductivity (Hamilton Conducell probe; Daqstation Yokogawa recorder) evolution after the injection of a NaCl solution (the tracer solution volume corresponds to 1% of the working volume of the reactor). In the case of SDR, injection has been performed at the level of the inlet of the non-mixed part and conductivity has been measured in the mixed part. In the case of the large-scale reactors, injection has been performed at the top of the vessel, and conductivity has been measured in the lower part of the vessel.

2.4. Biological tracer tests

Biological tracer experiments are performed in SDR type A by injecting a pulse of a solution containing stained cells in the bioreactor. The cells are stained with a fluorescent dye (Vybrant CFDA SE cell tracer kit V-12883), which permits to facilitate the detection by epifluorescent microscopy. The staining protocol consists in performing a preculture in a 500 ml Erlenmeyer flask, in order to obtain the required amount of biomass for further staining. An aliquot of the preculture is centrifuged (5 min at 4000 rpm). The precipitate is washed with 10 ml of sterile PBS buffer (NaCl 8 g/l; KCl 0.2 g/l; K_2HPO_4 1.44 g/l; KH_2PO_4 0.24 g/l; adjusted to pH 7.5 with K_2HPO_4 and KH_2PO_4). Three successive centrifugation/washing sequences are performed. After this step, microbial cells are stained by adding 1 mM of carboxyfluorescein diacetate succinimidyl ester (CFDA SE) followed by an incubation for 3 h at 30 °C. After the incubation, the solution is centrifuged and the precipitate is washed with PBS buffer. When performing a biological tracer

test, 5 ml of the stained cells suspension (2×10^8 cells/ml) are poured at the level of the non-mixed part of the SDR, and samplings are taken in of the mixed part. Cells are directly counted by fluorescent microscopy. For each sample, three aliquots of $10 \mu\text{l}$ each are placed on a microscopic plate for further counting. For each aliquot, three counts are performed, for three widths of the microscopic plate. Mean and standard deviation are calculated for each sample.

2.5. Scale-down fermentation experiments

S. cerevisiae (MUCL 43341) strain is stored at -80°C . Cultures are performed in a scale-down reactor including a 20 l stirred vessel ($D=0.22$ m) (Biolafitte-France) equipped with a RDT6 Rushton turbine ($d=0.1$ m) connected to a non-mixed part. The two non-mixed part design investigated in this study have been previously described in this material and methods section. Components of the culture media are: glucose 5 g/l, yeast extract 10 g/l and casein pepton 10 g/l. During the process, the broth is continuously recirculated between the stirred vessel (mixed part) and the non-mixed part by a peristaltic pump (Watson Marlow 323 S/D). The regulation of the culture parameters (pH, temperature, . . .) is ensured by a direct control system (ABB). Dissolved oxygen is maintained above 30% of saturation level by modulating the stirrer speed. Glucose addition is performed in the inlet of the non-mixed part and is controlled by an exponential feeding algorithm according to the equation $F = F_0 \exp(\mu t)$. With F being the feed flow rate (m^3/s), F_0 the initial feed flow rate (m^3/s), μ the microorganism growth rate (h^{-1}) and t is the culture time (h). The two parameters $\mu = 0.005 \text{ min}^{-1}$ and $F_0 = 0.086 \text{ ml/min}$ were calculated from growth data of *S. cerevisiae* in a batch bioreactor.

2.6. Stochastic modelling principles and distribution frequency calculation

The modelling strategy exposed is entirely based on stochastic processes. In fact, two sub-models are required: a first sub-model for the microbial cells circulation inside the bioreactor and a second one for the simulation of the gradient concentration. The advantage of the stochastic formulation lies in the fact that the two sub-models have the same structure based on the compartmentalization of the bioreactor. The principle is based on the tank-in-series concept and each compartment, representing a given zone in the bioreactor, is assumed to be perfectly mixed. In stochastic modelling, the displacements from one compartment to another are governed by probabilities. Fig. 1 presents the model structure used in the case of the SDR. The stirred vessel constituting the mixed part of the SDR has been modelled by eight vertical planes comprising each eight compartments. The compartments interconnections are in accordance with the radial flow developed by the rushton turbine used for the experiments.

The first sub-model describes the displacement of microorganisms inside the bioreactor. In this model, the displacement of a particle (e.g. a microbial cell or a tracer molecule) is calculated by comparison between a random number and the value

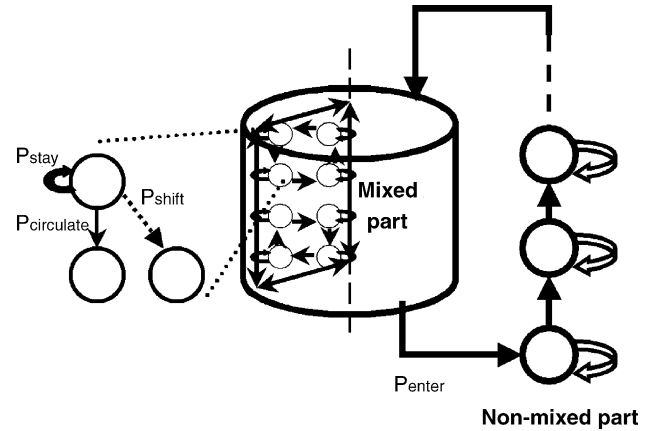


Fig. 1. Structure of the compartment model used to run stochastic simulations. In the case of the SDR type A, the non-mixed part comprises 3 compartments (with the volume of each compartment being 0.33 l), whereas in the case of SDR type B, there are 15 compartments (the volume of each compartment being equal to 0.03 l).

of the transition probabilities. Four kinds of probabilities are to be considered to describe the displacement of particles in the mixed part of the SDR: the probability to stay in a given circulation flow loop, the probability to stay in the same compartment, the probability to shift to another plane and the probability to switch from the main flow loop (this method has been proposed by ref. [13]). The circulation probability can be estimated from dimensionless correlation with the circulation flow rate, and is written as:

$$Q_c = N_{qc} N d^3 \quad (1)$$

where N_{qc} being a dimensionless number having a constant value in the turbulent flow regime and N being the impeller rotational speed (s^{-1}) and:

$$P_{\text{circulation}} = \frac{Q_c}{V_{\text{compartment}}} \Delta t \quad (2)$$

where Δt being the time interval between two transitions and $V_{\text{compartment}}$ the volume of a compartment in the model.

The switching probability express the level of turbulent mixing is written as:

$$P_{\text{switch}} = P_{\text{tangential}} = P_{\text{stay}} = \frac{1 - P_{\text{circulation}}}{3} \quad (3)$$

where P_{stay} being the probability to stay in the actual compartment, $P_{\text{tangential}}$ being the probability to shift to another plane and P_{switch} being the probability to shift from the main circulation flow loop.

In the case of a SDR, we also must express the probability for a particle to enter in the non-mixed part, which can be written as:

$$P_{\text{enter}} = \frac{Q_{\text{recirc}}}{V_{\text{compartment}}} \Delta t \quad (4)$$

where Q_{recirc} being the recirculation flow rate between the two parts of the SDR. The probabilities inside the non-mixed part are determined according to the recirculation flow rate and the respective compartment volume. All the transition probabilities

to pass from a compartment to another are collected in a transition matrix for computational ease.

The second sub-model is also based on the same transition matrix as the one used for the previous sub-model, but the dispersion of tracer molecules is here described by a Markov process. The Markov chain stochastic model consists of an initial state vector S_0 , which is multiplied with a transition matrix T to give a new state, S_1 . This procedure can be written as:

$$\text{for the first transition : } S_1 = TS_0 \quad (5)$$

The next stage involves the multiplication of the new state vector S_1 with the same transition matrix T until a steady-state is reached:

the second transition can be written as : ($S_2 = TS_1$)

$$\text{or } (S_2 = T^2 S_0), \quad (6)$$

and the i th transition : ($S_i = TS_{i-1}$) or ($S_i = T^i S_0$) (7)

In our case, the state vector represents the tracer concentration values for all compartments. In order to obtain a valuable insight into the concentration field evolution during the bioprocess, the pulse effect of the feed pump must be taken into account. In our case, the pulse frequency is time varying because of the exponential increase of the feed flow rate during the culture. This pulse frequency can be included in the stochastic model by the use of the following matrix:

$$S_{\text{pulse}} = \begin{bmatrix} C_{\text{pulse}} & 0 & 0 & 0 & C_{\text{pulse}} & 0 \\ 0 & \cdot & \cdot & \cdot & \cdot & \cdot \\ \cdot & \cdot & \cdot & \cdot & \cdot & \cdot \\ \cdot & \cdot & \cdot & \cdot & \cdot & \cdot \\ \cdot & \cdot & \cdot & \cdot & \cdot & \cdot \\ \cdot & \cdot & \cdot & \cdot & \cdot & \cdot \\ 0 & 0 & 0 & \cdot & \cdot & 0 \end{bmatrix} \quad (8)$$

In the first row, the number of zero elements between two pulses (C_{pulse} being the concentration of the tracer pulse) depends of the feed pump activation frequency. The number

of elements in a column corresponds to the number of compartments in the model. In the case of this matrix, the pulse is added at the level of the first state of the model (first element in a column). The number of elements in a row corresponds to the number of simulation steps performed.

The matrix S_{pulse} is used as follow to describe the evolution of the state vector:

$$S_i = TS_{i-1} + S_{\text{pulse}} \quad (9)$$

The strategy adopted here is to superimpose the gradient field obtained with the Markov chain model on the microorganisms circulation process obtained with the classical stochastic model, in order to obtain the concentration profile experienced by a population comprising a given number of microorganisms.

The superimposition results are expressed in terms of frequency distribution of the mean relative concentrations experienced by the microorganisms. The frequency distributions calculated here are used to characterize the environment heterogeneity experienced by a microbial population of n cells on a time interval t for a given set of operating conditions and bioreactor configurations.

3. Results and discussion

3.1. Validation of the fluid mixing (Markov chain) and of the circulation (random number) models

Concentration gradient inside SDR is modelled by a stochastic Markov chain procedure. The non-mixed part of the SDR type A has simply been modelled by three compartments in series. This is justified by the strong dispersing effect that perturbs the establishment of a nearly plug-flow in this part of the reactor. Comparison between the experimental inert tracer test and the simulation results is shown in Fig. 2A.

In the case of the SDR type B, due to the strong plug-flow exhibited by the non-mixed part, the number of compartments in this section of the reactor has been increased. Different numbers of compartments have been used to model this part of the SDR. The best results are been obtained with 15 compartments in series. Comparison between the simulation and the experimental

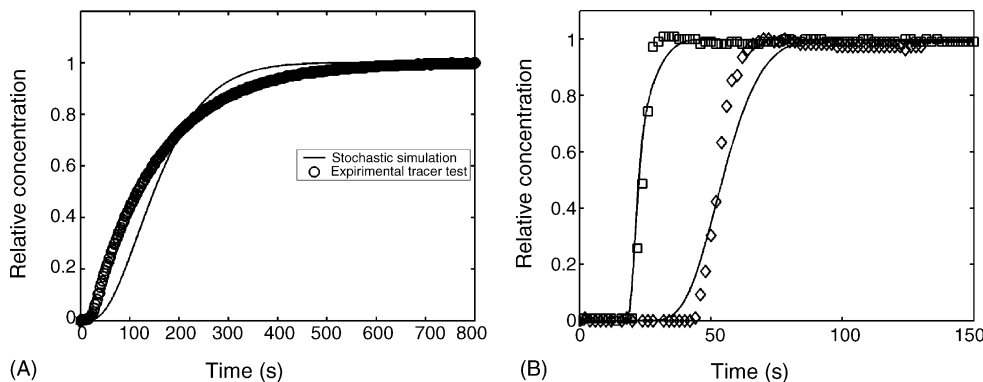


Fig. 2. Comparison of experimental tracer curve and stochastic (Markov chain) simulations results. (A) SDR type A ($Q_{\text{recirc}} = 18$ l/h); (B) SDR type B (\square : $Q_{\text{recirc}} = 18$ l/h; \diamond : $Q_{\text{recirc}} = 39$ l/h).

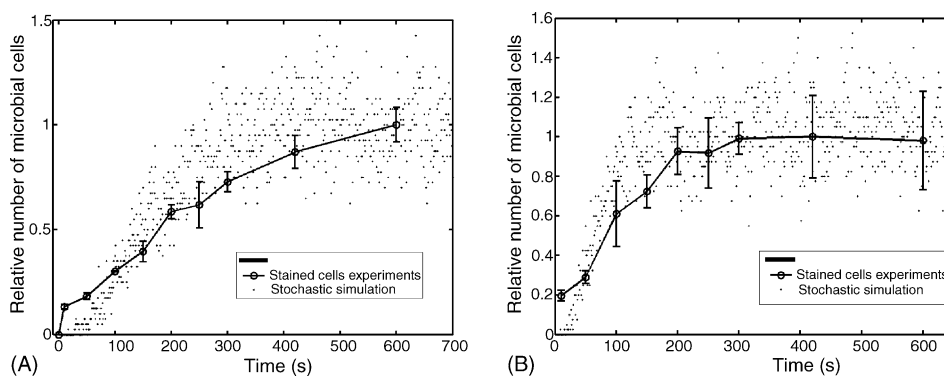


Fig. 3. Comparison of biological tracer tests with stochastic non-Markov microbial cells dispersion simulations in SDR. (A) SDR type A $Q_{\text{recirc}} = 18$ l/h; (B) SDR type A $Q_{\text{recirc}} = 39$ l/h.

tracer test is shown in Fig. 2B. The results show that there is a good agreement between the Markov chain simulations and the experimental results.

Fig. 2 reveals fundamental differences between the hydrodynamics developed by the SDR types A and B. This suggests that the scale-down effect will also be different. This important point will be analysed by using the stochastic modelling methodology presented in this study.

In order to follow the dispersion of a microbial population inside a bioreactor and thus to validate the circulation stochastic model, biological tracer tests are performed on the SDR type A, to validate the simulation results obtained by the stochastic non-Markov model (Fig. 3).

Fig. 3 shows that both the experimental and simulation results show strong variations. Variations are more pronounced for the simulation results than for the experimental ones. Two explanations are possible. Firstly, the number of microbial cells used to perform simulations is not high enough and the stochasticity impact is thus very important. In order to decrease the fluctuations, the number of microbial cells used to run simulations must be increased, but in this case the computational time is increased too. Secondly, only three repetitions per sample have been performed during the biological tracer tests. Increasing the number of repetitions can increase the standard deviation on each sample.

However, the same general trend is observed for the experimental results as well as for the simulation ones. We can thus assume that the model is reliable enough to perform our microbial cells dispersion simulations.

3.2. Characterization of the concentration profiles experienced by the microbial cells

In the following sections, the stochastic bioreactor modelling methodology will be improved, mainly in taking account of the influence of several parameters on the final concentration frequency distributions.

3.2.1. Effect of the glucose pulses frequency

During a fed-batch culture under exponential control of the substrate addition into the reactor, the pulse frequency of the feed pump is exponentially increasing until reaching a constant

level at the end of the culture, to prevent glucose overflow. In the earlier stage of the exponential feed profile, glucose pulses are very spaced and the transient mixing behaviour of the system is sufficient to reach an acceptable degree of homogeneity during the time interval separating two successive pulses. In the final stage of the exponential feed profile, pulses are less and less spaced and a stable concentration gradient thus appears.

The frequency distribution is calculated from simulations performed in a scale-down system A, with a recirculation flow rate of 39 l/h, these simulations involving 3500 microbial cells starting from the non-mixed part (Fig. 4). These simulations show that the pulse profile of the feed pump greatly influences the frequency distribution of the mean concentration experienced by the microorganisms in the bioreactor:

- For a time interval between two pulses (T_{pulse}) smaller than the global mixing time of the system (Fig. 4A), the mean concentrations experienced by the microorganisms are very low. About 60% of the microbial population is exposed to a mean relative concentration centered on a relative intensity of 0. This is due to the fact that, between two pulses, the concentration gradient at the level of the mixed part of the SDR disappears.
- For T_{pulse} approximately equal to the mixing time of the scale-down reactor, Fig. 4B shows that a concentration gradient is maintained. This concentration gradient persistence leads to the increase of the mean concentration experienced by the microorganisms, as well as an increase of the variance of the frequency distribution.
- For T_{pulse} inferior to the mixing time of the SDR (Fig. 4C), these observations are maintained, with a new increase both of the mean relative concentration experienced and of the variance of the frequency distribution.
- For T_{pulse} smaller than the mixing time related to the mixed part of the SDR (Fig. 4D), there is also establishment of a gradient in this part of the reactor.

Fig. 4 clearly shows the critical phase of the fed-batch culture, corresponding to the case 4D, displaying the most dispersed frequency distribution. For the next calculations, this stage of the fed-batch culture will consequently be used.

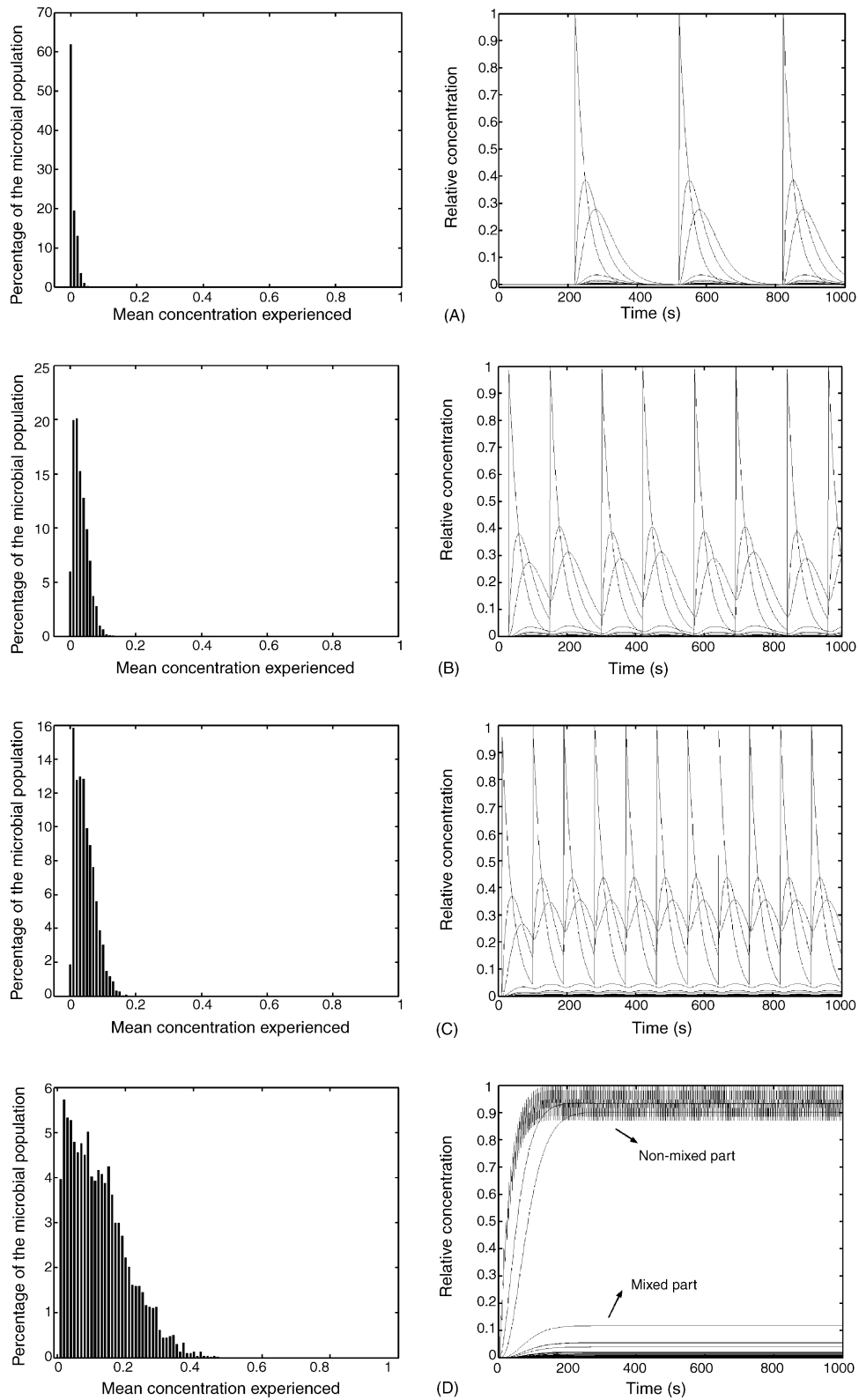


Fig. 4. Evolution of the distribution frequency in function of the evolution of the feed pump frequency during a fed-batch culture in a SDR type A working at $Q_{\text{recirc}} = 39$ l/h with the tracked microbial population starting from the non-mixed part of the reactor. (A) Moderate pulse frequency corresponding to the earlier stage of a fed-batch culture; (B) pulse frequency approaching the mixing time of the reactor; (C) pulse frequency inferior to the mixing time of the reactor; (D) constant pulse frequency of 5 s. For each distribution, the relative concentration profile is presented at the right side.

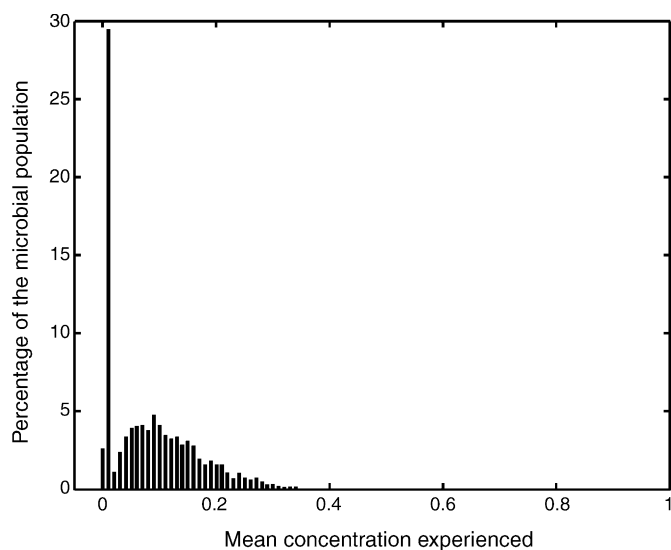


Fig. 5. Distribution frequency obtained with a SDR type A ($Q_{\text{recirc}} = 39$ l/h) with a microbial population starting from the mixed part of the reactor.

3.2.2. Effect of the initial position of the tracked microbial population and of the exposure time

By considering the initial position of the microorganisms in the SDR, two kinds of simulation can be run. Firstly, a simulation involving an initial position located at the level of the mixed part of the SDR, and secondly a simulation involving an initial position located at the level of the non-mixed part of the SDR. Since the feed addition is performed at the level of the non-mixed part inlet, differences can occur when comparing the respective frequency distributions. Indeed, if compared with Fig. 4D, which shows the frequency distribution obtained under the same operating conditions but with population starting from the non-mixed part, Fig. 5 shows that about 30% of the microbial population are submitted to very low extracellular concentration.

When performing a simulation with an initial position corresponding to the non-mixed part, each microorganism is exposed at least one time to high extracellular concentration fluctuations. This is not the case of those starting from the mixed part of the SDR, for which the shape of the frequency distribution is greatly

influenced by the probability to enter in the non-mixed section. In this context, it is interesting to analyse the influence of the simulation time.

Fig. 6 shows that when increasing the simulation time, the shapes of the frequency distributions are very similar for the two initial positions. This fact suggests that, for a sufficiently long simulation time, the initial position of the tracked microbial population can be assumed to have no influence on the shape of the frequency distribution.

3.2.3. Effect of the microbial population size

It is also important to determine if the amount of microbial cells considered in the simulations is sufficient to give a valuable insight into the behaviour of the whole population. Fig. 7 shows the frequency distribution corresponding to population sizes of, respectively, 1000 and 10,000 microbial cells.

When considering a population of 1000 microbial cells (Fig. 7A), the corresponding distribution frequency displays slight differences compared with the one involving a larger amount of cells (Figs. 7B and 4D). However, in the case of a population of 10,000 cells (Fig. 7B), no significant difference appears, compared with the results obtained for a limited population of 3500 microbial cells (Fig. 4D). Considering the large computational time required for microbial population comprising a large number of cells, only 3500 cells will be taken in account for the next simulations. Indeed, it takes about one hour to simulate the displacement of 10,000 cells for 1000 s by using a Pentium 4 2 GHz processor, the computational time being directly proportional to the number of cells and to the exposure time.

3.3. Application to the analysis of fermentation tests carried out in SDR

In order to improve the modelling methodology involved in this study, some fermentation tests were carried out in SDR, for different operating conditions and for different non-mixed part geometry. The results are presented in Fig. 8 and show a better biomass yield in the case of a classical stirred bioreactor than for the SDRs.

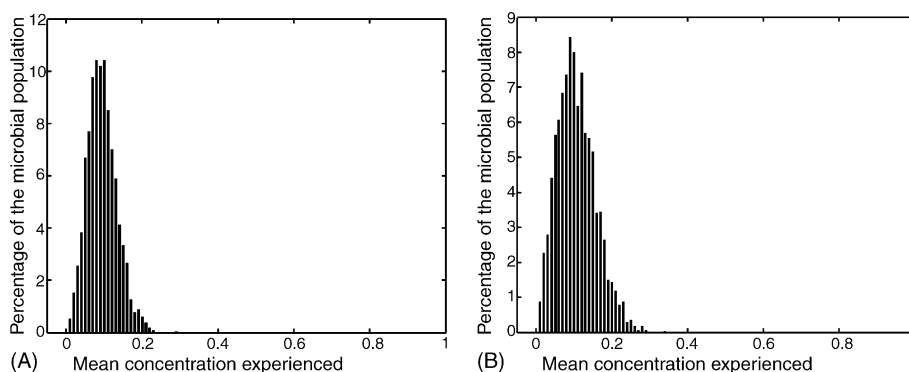


Fig. 6. Frequency distributions obtained (A) for a microbial population starting from the mixed part of the SDR and with an exposure time of 5000 s. (B) For a microbial population starting from the non-mixed part of the SDR and with an exposure time of 3000 s (for the two experiments: SDR type A; 39 l/h; 3500 microbial cells involved).

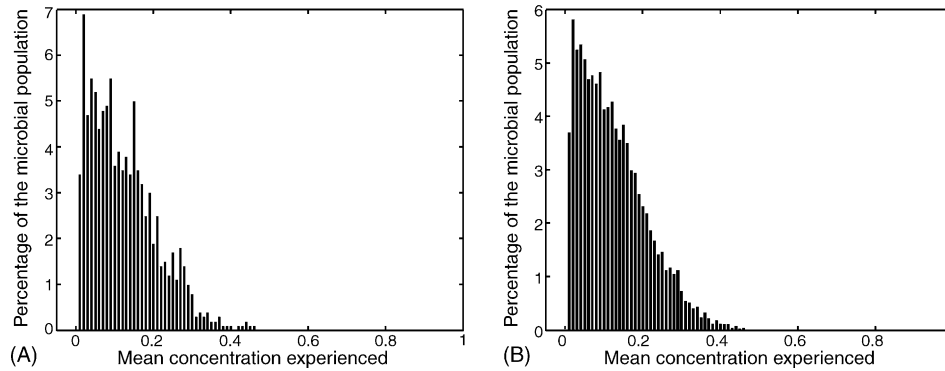


Fig. 7. Distribution frequency obtained with a SDR type A ($Q_{\text{recirc}} = 391/\text{h}$), for an exposure time of 1000 s to a glucose pulse profile ($T_{\text{pulse}} = 5$ s). The microbial population comprises, respectively, 1000 cells (A) and 10,000 cells (B).

For each fermentation test, a stochastic simulation is performed in order to calculate the corresponding relative concentration frequency distribution. The simulations are performed by considering 3500 microorganisms, for a time interval of 5000 s. The initial location of the microbial population in the model is the mixed part of the reactor, but a previous analysis has shown that this parameter has no impact if the exposure time is sufficiently long.

In the case of the SDR type A, Fig. 8 reveals a clear impact of the recirculation flow rate between the mixed and the non-mixed part of the reactor. Increasing the recirculation flow rate induces an increase of the biomass yield. The frequency distributions presented in Fig. 9 validate this observation. Indeed, it is to be noted that, when increasing the recirculation flow rate, there is a shift of the distribution to the left, which means that the microorganisms are exposed to less elevated extracellular substrate concentrations. This is also true in the case of the SDR type B (Fig. 9C and B). Nevertheless, the biomass yield is very low for the two recirculation flow rates investigated in the case of the SDR type B (Fig. 8). On the other hand, analysis of the respective frequency distributions reveals better hydrodynamic conditions than for the SDR type A, but this fact is not confirmed

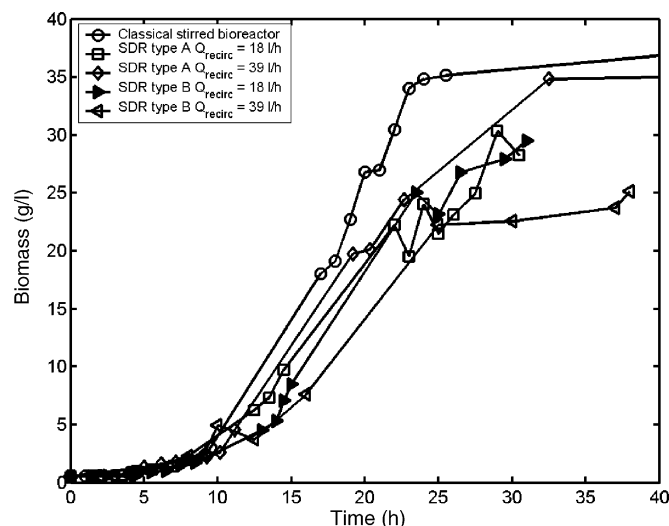


Fig. 8. Microbial growth curves obtained from classical and scale-down stirred bioreactors.

by fermentation experiments. Fig. 10 shows that the exposure mechanisms in the SDR type A and for the type B are quite different. In the case of the SDR type B, microorganisms are subjected to large extracellular substrate relative concentration exceeding unity, whereas in the case of the SDR type A these fluctuations are less intensive but more extended on time. These differences can be attributed to the respective design of the non-mixed part of each SDR.

The impact of such fluctuations on the physiology and growth of *S. cerevisiae* is not actually well understood, but an hypothetical mechanism can be proposed. Indeed, a previous study as proven the capability of *S. cerevisiae* to adapt its glucose metabolism when submitted to repeated glucose pulses [14]. The authors highlight the fact that the time scale involved at the level of the microorganism exposure frequency to extracellular glucose fluctuations might have drastic implications for the metabolic performance of the cells and for their gene expression patterns. Fig. 10 shows that two distinct exposure mechanisms are observed in function of the kind of SDR used. For the SDR type A, a microorganism entering in the non-mixed part is submitted to a fluctuating extracellular environment maintained for a relatively long time, whereas in the case of the SDR type B, these fluctuations are not maintained for a long time but are more frequent and more intensive. It can be assumed, on the basis of the previously described work [14], that microbial cells travelling in SDR type A are more adapted to a fluctuating extracellular environment than in the case of the SDR type B.

The connection of the stochastic hydrodynamic model presented in this study with a microbial kinetic model would be helpful to investigate the impact of the extracellular environment on the microorganisms physiology.

3.4. Are the SDR frequency distributions representative of those calculated for the large-scale reactors?

All the previous frequency distributions are valid in the case of a SDR. But, are these distributions representative of a large-scale stirred bioreactor? The following simulations have been performed on the basis of mixing time experiments in 2 m^3 three-staged bioreactor. This reactor has been modelled on the same basis than the SDR but without non-mixed part. The 2 m^3

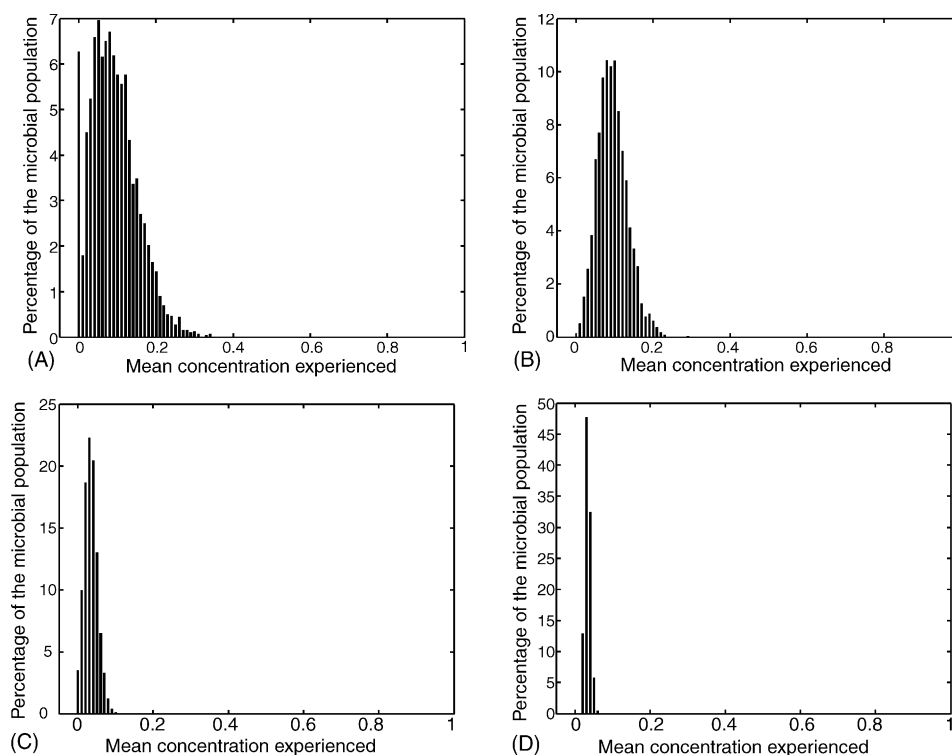


Fig. 9. Frequency distributions obtained in the case of: (A) a SDR type A $Q_{\text{recirc}} = 18$ l/h; (B) a SDR type A $Q_{\text{recirc}} = 39$ l/h; (C) a SDR type B $Q_{\text{recirc}} = 18$ l/h; (D) a SDR type B $Q_{\text{recirc}} = 39$ l/h. All the simulations involve a population of 3500 microorganisms for 5000 s.

reactor comprises three agitation stages and the compartment arrangement for one agitation stage corresponds to the one of the mixed part of the SDR (Fig. 1). The volume of each compartment too has been modified to give a global volume of 1800 l (which corresponds to the working volume of the 2 m³ reactor). The transitions between the agitation stages have been assumed to correspond to switching probabilities (Eq. (3)). In the case of a 9 m³ bubble column ($D=2$ m), we assumed an axial liquid circulation flow pattern. Due to the height to diameter ratio (1.5:1) of this apparatus, the compartments network of Fig. 1 has been modified in eight planes comprising each 12 compartments. In addition, the circulation transition probabilities orientation have been modified to be in accordance with an axial flow pattern. Liquid mixing in bubble columns is induced by the rise of bubbles through the liquid phase. The circulation flow rate can thus be calculated in function of the air

flow rate. In this study, a correlation previously used by Zahradnik et al. [4] for a determinist compartments network has been selected:

$$Q_c = \left[\frac{Du_g(\rho_l - \rho_g)}{2.5\rho_l} \right]^{1/3} \quad (10)$$

where D being the reactor diameter (m), u_{sg} the gas superficial velocity (m/s), ρ_l the liquid density (kg/m³) and ρ_g is the gas density (kg/m³). In our case, the air is dispersed by a multi-pipe sparger (holes diameter: 3 mm) placed to cover the entire section of the reactor.

For all the large-scale simulations, the concentration gradient sub-model has been validated by inert tracer tests. In the case of the microorganisms circulation sub-model, the assumption has been made that fluid mixing-particle circulation equivalency applies too in the case of large-scale reactors (the realization of

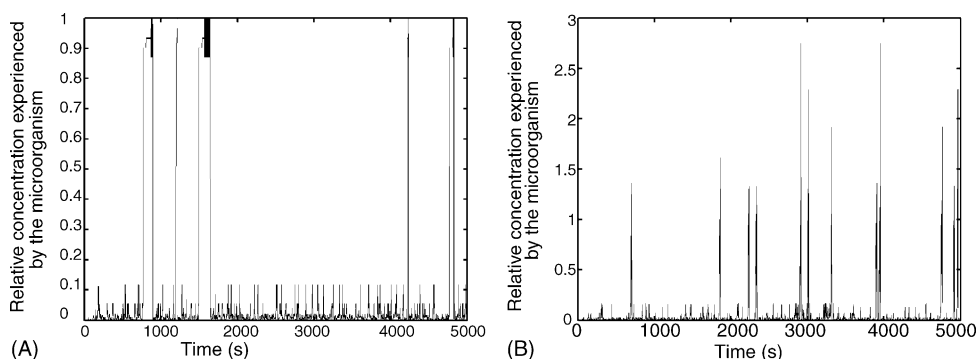


Fig. 10. Sample path of the stochastic displacement of a microorganism in: (A) a SDR type A; (B) a SDR type B ($Q_{\text{recirc}} = 39$ l/h).

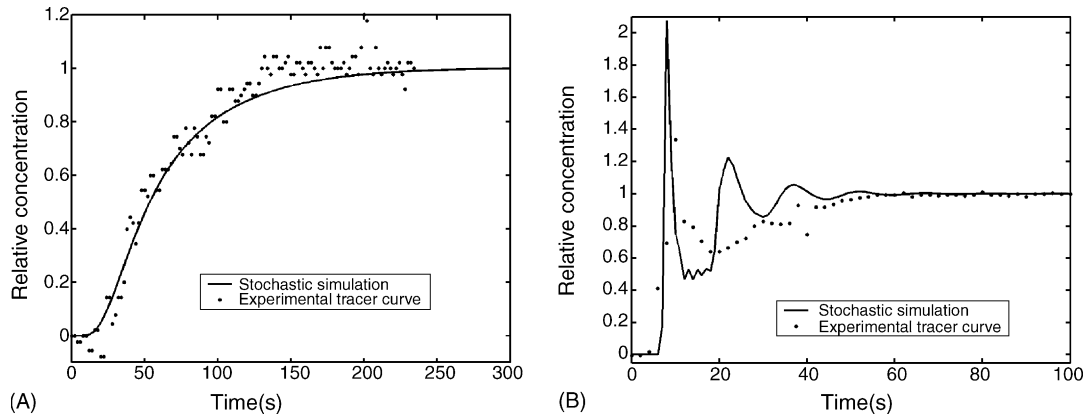


Fig. 11. Simulated and experimental tracer curve for large-scale bioreactors (probe located at the bottom part of the reactor in each case). (A) Two cubic metre three-staged (RDT6) stirred bioreactor operating at 38 rpm. (B) Nine cubic metre bubble column operating at an air flow rate of $66 \text{ m}^3/\text{h}$.

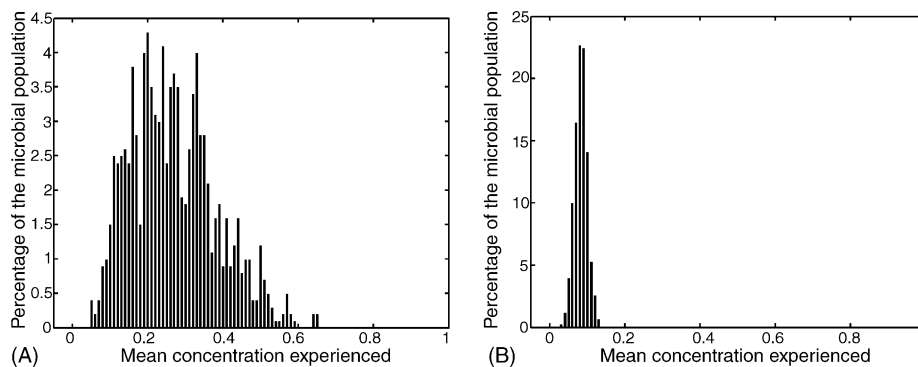


Fig. 12. Distribution frequency obtained in the case of large-scale bioreactors. (A) Two cubic metre three-staged (RDT6) stirred bioreactor operating at 38 rpm. (B) Nine cubic metre bubble column operating at an air flow rate of $66 \text{ m}^3/\text{h}$.

the biological tracer tests being hard to be realized on this kind of apparatus).

On the basis of the homogenization efficiency, Figs. 11B and 12B show that the bubble column reactor is better. But this comparison has not been performed at the same power input. Indeed, the stirred bioreactor operate at very low stirrer speed (38 rpm) which explains the poor mixing efficiency. The reason governing the choice of such a low stirrer speed is that the 2 m^3 is a pilot scale reactor not very representative of an industrial scale reactor. In order to enhance the compartmentalization impact in the 2 m^3 reactor, the stirrer speed (and thus the power input) has been lowered. In the case of the bubble column reactor, it was not possible to lower the air flow rate below $66 \text{ m}^3/\text{h}$. The goal of the approach used here is to compare the large-scale hydrodynamic behaviour of a pneumatic reactor and a mechanically stirred reactor. In this context, Fig. 12 shows strong differences in terms of behaviour between the 2 m^3 stirred bioreactor and the 9 m^3 bubble column hydrodynamics. Indeed, the frequency distribution shows a more dispersed behaviour in the case of the stirred bioreactor. This can be explained by the flow compartmentalization induced by the three radial impellers delimiting three distinct agitation stages. It is interesting to note that the frequency distribution presents some similarities with those of the SDR type A. In the case of the bubble column, the distribution is mainly centered on the mean. This is due to the strong circu-

lation induced by the ascending bubbles in the whole volume of the reactor. As opposed to the stirred bioreactor, it can be said that the behaviour of the bubble column can be approached by the SDR type B. These observations point out the fact that the non-mixed part design of SDR can be arranged in such fashion to reproduce efficiently the extracellular environment experienced by the microorganisms in displacement in a given large-scale reactor.

In this section, simulation results relative to large-scale reactors have been presented. However, in large-scale reactors, the possible paths that can be taken by the circulating microorganisms are numerous. A more refined model structure (obtained by increasing the number of compartments and by considering concentric flow loops [15]) would lead to better results, in the sense that the circulation time distribution is affected by the number of compartments of the stochastic model.

4. Conclusions

A stochastic structured model has been elaborated in order to analyse both fluid mixing and microorganisms displacement dynamics in bioreactors. The superimposition of the concentration gradient on the microorganisms circulation paths has allowed to obtain the characteristic concentration profiles encountered in the bioreactor. The results are presented on the

form of frequency distribution of the mean relative concentration experienced by microorganisms. It has been shown that these distributions reflect the mixing and circulation efficiency of a bioreactor, in connection with the microorganism exposure to gradient stress.

Several parameters being able to have an impact on the distributions have been tested. It has to be noted that the pulse frequency of the feed pump in a fed-batch context, the exposure time and the initial location of the microorganisms in the reactor have a significant influence on the shape of the distributions. For a sufficient exposure time (5000 s), simulations have shown that the initial location of the tracked population has no impact on the results. The design of the non-mixed part of the SDR too has a great impact on the frequency. Indeed, the frequency distributions analysis provides valuable insights into the biomass yield differences obtained if increasing or decreasing the recirculation flow rate in the case of the fermentation tests performed in SDR, but cannot provide any explanation about the differences observed between the SDR type A and the SDR type B. This suggests that two distinct mechanisms for the microorganisms exposure to gradient stress have to be considered, the hydrodynamics generated by the SDR type A allowing the adaptation of microbial cells to a fluctuating extracellular environment.

The analysis of the distributions reveals that several microbial sub-populations can be distinguished, differing by the extracellular substrate concentrations experienced. In the perspective to elucidate the stress mechanisms induced by the bioreactor hydrodynamic performances, it should be interesting to distinguish clearly these different sub-populations, by considering, for example, transition values of mean relative concentration experienced. This is not an easy task since each microbial strain has its own sensibility to concentration gradient. To be able to study these transitions between sub-populations, the elaboration of a microbial growth model taking into account the respective flow history of each cell, can be an efficient method. In this context, the stochastic methodology presented in this study could constitute the first step in the elaboration of a reliable microbial kinetic model. Nevertheless, there is a lack about the size of the observed microbial population. In our simulations, this size was not exceeding 10,000 microbial cells, whereas about 10^8 – 10^9 microbial cells per ml of broth have in fact to be considered. This fact could disturb the representativeness of the frequency distributions, but considering such a large microbial population is not quite possible due to the excessive computational time this would take.

In another perspective, other sources of heterogeneities can be studied by the methodology presented in this paper. For example, the oxygen gradient impact on the microbial population growth can be studied by this way [16].

Acknowledgements

The authors gratefully acknowledge Mr. P. De Pauw and Mr. C. Vermeulen from the Puratos group (Beldem), as well as Mr. P. Evrard from THT S.A. for the access to the large-scale fermentation equipments.

References

- [1] P. Neubauer, L. Horvat, S.O. Enfors, Influence of substrate oscillations on acetate formation and growth yield in *Escherichia coli* glucose limited fed-batch cultivations, *Biotechnol. Bioeng.* 47 (1995) 139–146.
- [2] B. Mayr, E. Nagy, P. Horvat, A. Moser, Scale-up on basis of structured mixing models: a new concept, *Biotechnol. Bioeng.* 43 (1994) 195–206.
- [3] B. Mayr, E. Nagy, P. Horvat, A. Moser, Modelling of mixing and simulation of its effect on glutamic acid fermentation, *Chem. Biochem. Eng. Q.* 7 (1) (1993) 31–42.
- [4] J. Zahradnik, R. Mann, M. Fialova, D. Vlaev, S.D. Vlaev, V. Lossev, P. Seichter, A network-of-zones analysis of mixing and mass transfer in three industrial bioreactors, *Chem. Eng. Sci.* 56 (2001) 485–492.
- [5] D. Vlaev, R. Mann, V. Lossev, S.D. Vlaev, J. Zahradnik, P. Seichter, Macro-mixing and *Streptomyces fradiae*: modelling oxygen and nutrient segregation in an industrial bioreactor, *Trans. IChemE* 78 (2000) 354–362.
- [6] H. Berthiaux, J. Dodds, Modeling classifier networks by Markov chains, *Powder Technol.* 105 (1999) 266–273.
- [7] H. Berthiaux, Analysis of grinding processes by Markov chains, *Chem. Eng. Sci.* 55 (2000) 4117–4127.
- [8] F. Delvigne, J. Destain, P. Thonart, Structured mixing model for stirred bioreactor: an extension to the stochastic approach, *Chem. Eng. J.* 113 (2005) 1–12.
- [9] B. Xu, M. Jahic, G. Blomsten, S.O. Enfors, Glucose overflow metabolism and mixed-acid fermentation in aerobic large-scale fed-batch processes with *Escherichia coli*, *Appl. Microbiol. Biotechnol.* 51 (1999) 564–571.
- [10] P.K. Namdev, B.G. Thompson, M.R. Gray, Effect of feed zone in fed-batch fermentations of *Saccharomyces cerevisiae*, *Biotechnol. Bioeng.* 40 (2) (1992) 235–246.
- [11] S. George, G. Larsson, K. Olsson, S.O. Enfors, Comparison of the Baker's yeast performance in laboratory and production scale, *Bioprocess Eng.* 18 (1998) 135–142.
- [12] J.D. Fowler, E.H. Dunlop, Effects of reactant heterogeneity and mixing on catabolite repression in cultures of *Saccharomyces cerevisiae*, *Biotechnol. Bioeng.* 33 (1989) 1039–1046.
- [13] R. Mann, P.P. Mavros, J.C. Middleton, A structured stochastic flow model for interpreting flow-follower data from a stirred vessel, *Trans. IChemE* 59 (1981) 271–278.
- [14] K.A. Reijenga, B.M. Bakker, C.C. van der Weijden, H.V. Westerhoff, Training of yeast cell dynamics, *FEBS J.* 272 (2005) 1616–1624.
- [15] R. Mann, S.K. Pillai, A.M. El-Hamouz, P. Ying, A. Togatorop, R.B. Edwards, Computational fluid mixing for stirred vessels: progress from seeing to believing, *Chem. Eng. J.* 59 (1995) 39–50.
- [16] R. Mann, D. Vlaev, V. Lossev, S.D. Vlaev, J. Zahradnik, P. Seichter, A network-of-zones analysis of the fundamentals of gas–liquid mixing in an industrial stirred bioreactor, *Récents progrès en génie des procédés* 11 (52) (1997) 223–230.